

## Titre

# Primary and secondary instabilities of viscoelastic fluids saturating a horizontal porous layer heated from below by a constant flux.

A. GUEYE<sup>a</sup>, H. BEN HAMED<sup>a</sup>, M.N. OUARZAZI<sup>b</sup>, S. HIRATA<sup>b</sup>

Laboratoire des Technologies Innovantes (LTI), Université de Picardie Jules Verne, IUT d'Amiens,  
Avenue des Facultés-Le Bailly 80025 Amiens Cedex, France abdoulaye.gueye@u-picardie.fr  
Laboratoire de Mécanique de Lille (LML), Université Lille 1-Sciences et technologies, Avenue Paul  
Langevin, 59650 Villeneuve d'Ascq, France najib.ouarzazi@univ-lille1.fr

...

## Abstract :

*Analytical and Numerical study of the primary and secondary instabilities of viscoelastic fluids saturating an horizontal porous layer heated by a constant flux is proposed in the present work. The mathematical formulation of the problem is based on the phenomenological law of Darcy generalized to a viscoelastic fluid verifying the Boussinesq approximation. This formulation introduces two additional parameters related to viscoelasticity, namely the relaxation time  $\lambda_1$  and the ratio  $Rv$  between the viscosity of the solvent and the total viscosity of the polymer solution. When the horizontal walls are considered perfectly conductive of heat, the linear and weakly nonlinear stability study has been carried out by Hirata et al. [1]. In the case when the horizontal boundaries are maintained at a constant flux, the linear stability analysis conducted in this work shows that the state of conduction loses its stability in favor of convective structures with different spatio-temporal properties depending on the viscoelastic parameters  $\lambda_1$  and  $Rv$ . In the  $(Rv, \lambda_1)$  plane, we identified two distinct regions. In a weakly viscoelastic regime, these convective structures have a stationary character where the most amplified mode is characterized by a long wavelength and the viscoelastic fluid behaves like a Newtonian fluid. However, it is shown that for strongly viscoelastic fluids, a Hopf bifurcation appears leading to oscillatory convective flows with a finite wave number and finite frequency. For weakly viscoelastic fluids, the parallel flow approximation is first used to determine the analytical solution of the unicellular flow convection in the nonlinear regime. In a second part, we perform a stability analysis of the unicellular flow convection for both Newtonien fluids and viscoelastic fluids against perturbations in the form of moving transverse rolls (TR), whose axis is perpendicular to the direction of the main flow. For Newtonian fluids, it is found that the critical Rayleigh number and the critical frequency corresponding to the appearance of multicellular flow in the form of TR are in excellent agreement with the values found in [2]. In the case of viscoelastic fluids, the threshold of the appearance of the secondary instabilities is determined and demonstrates the destabilizing effect of the viscoelastic character of the fluid.*

**Mots clefs : Instability, Viscoelastic fluids, Porous media, Convection**

## 1 Introduction

The study of viscoelastic fluids have applications in a number of processes that occur in industry, such as the extrusion of polymer fluids, solidification of liquid crystals, suspension solutions and petroleum activities. In contrast to the case of Newtonian fluids, study of thermal convection of viscoelastic fluids in porous media is limited. In rheology, one crucial problem is the formulation of the constitutive equations regarding viscoelastic fluid flows in porous media. Recently, a modified Darcy's law was employed to study the stability of a viscoelastic fluid in a horizontal porous layer using linear and nonlinear stability theory ([3]-[8]). Kim et al. [3] and Yoon et al. [4] performed a linear stability analysis and showed that in viscoelastic fluids such as polymeric liquids, a Hopf bifurcation as well as a stationary bifurcation may occur depending on the magnitude of the viscoelastic parameter. From the nonlinear point of view, Kim et al. [3] carried out a nonlinear stability analysis by assuming a densely packed porous layer and found that both stationary and Hopf bifurcations are supercritical relative to the critical heating rate. The question of whether standing or traveling waves are preferred at onset has been fully addressed by Hirata et al. [1]. The three-dimensional convective and absolute instabilities of a viscoelastic fluid in presence of a horizontal pressure gradient have been analyzed by Hirata and Ouarzazi [5]. Alves et al. [6] studied the effect of viscous dissipation of viscoelastic fluids at the onset of convection. In addition to its theoretical interest, Delenda et al [7] have showed that viscoelastic convection in porous media may be useful for industrial applications interested by the separation of species of viscoelastic solutions. All the above investigations considered conventional boundary conditions, namely impermeable isothermal horizontal plates and impermeable adiabatic side walls, commonly known as Horton-Rogers-Lapwood convection. However, to the best of our knowledge, no results have been published for thermal convection of viscoelastic fluids when the porous medium is heated from below and cooled from above with a constant heat flux. Therefore, the objective of this work is to fill this gap by investigating the primary and secondary instabilities of viscoelastic fluids under the assumption that the upper and lower horizontal walls are impermeable and are kept at a constant flux, while the lateral vertical walls are considered impermeable and adiabatic.

Therefore, this work may be viewed as an extension to viscoelastic fluids of the work done by Kimura et al. [2].

## 2 Mathematical formulation

Let us consider an isotropic and homogeneous porous cavity of thickness  $e$ , height  $H$ , width  $W$ . The porous medium is saturated by an Oldroyd-B fluid and we assume that the solid matrix is in local thermal equilibrium with the fluid. The upper and lower horizontal walls are kept at constant flux, while the lateral vertical walls are considered adiabatic. The solid walls of the domain  $\Omega = [0, W] \times [0, e] \times [0, H]$  are considered impermeable. We assume that the Oberbeck-Boussinesq approximation holds.

There are several ways to obtain macroscopic laws for polymeric flows in a porous medium : by direct numerical simulations of viscoelastic flows in a specific pore geometry model (a good review of these studies can be found in [10]) or analytical ways. In general, the former is the most commonly used way for the derivation of macroscopic laws. It can be divided in two techniques : the REV method (representative elementary volume method) and the homogenization theory. The starting point for the two techniques is a local description in a pore scale. The pore space is assumed to be saturated by an incompressible viscoelastic fluid. For slow flows, the momentum balance equation can be linearized :

$$\rho \frac{\partial \mathbf{U}^*}{\partial t^*} = -\nabla p^* + \rho \mathbf{g} + \nabla \cdot \tilde{\tau} \quad (1)$$

where  $\mathbf{U}^*$  is the fluid velocity field,  $p^*$  is the pressure,  $\tilde{\tau}$  is the stress tensor and  $\mathbf{g}$  is the gravity field.

In Newtonian incompressible fluids, the constitutive relation between stress tensor  $\tilde{\tau}$  and strain tensor  $\tilde{D}$  ( $D_{i,j} = [u_{i,j}^* + u_{j,i}^*]/2$ ) is the Newtonian law  $\tilde{\tau} = 2 \mu_N \tilde{D}$ , where  $\mu_N$  is the dynamic viscosity, and, in this case, the relation  $\nabla \cdot \tilde{\tau} = \mu_N \nabla^2 \mathbf{U}^*$  is obtained.

The rheological model relating  $\tilde{\tau}$  and  $\tilde{D}$  for viscoelastic fluids, such as a polymeric solution composed of a Newtonian solvent and a polymeric solute of "Newtonian" viscosity  $\mu_s$  and "elastic viscosity"  $\mu_p$  [11] respectively, is given by :

$$\tilde{\tau} = \tilde{\tau}_s + \tilde{\tau}_p \quad (2)$$

with

$$\tilde{\tau}_s = 2 \mu_s \tilde{D} \quad (3)$$

and

$$(1 + \lambda_1^* \frac{\partial}{\partial t^*}) \tilde{\tau}_p = 2 \mu_p \tilde{D} \quad (4)$$

where  $\lambda_1^*$  represents the relaxation time. Then, by combining 2-4 we obtain the constitutive equation :

$$(1 + \lambda_1^* \frac{\partial}{\partial t^*}) \tilde{\tau}_p = 2 \mu (1 + \lambda_2^* \frac{\partial}{\partial t^*}) \tilde{D} \quad (5)$$

where the dynamic viscosity  $\mu$  and the retardation time  $\lambda_2^*$  are related to  $\mu_s$  and  $\mu_p$  by :

$$\mu = \mu_s + \mu_p \quad \text{and} \quad \lambda_2^*/\lambda_1^* = \mu_s/(\mu_s + \mu_p).$$

An Oldroyd-b fluid may thus be characterized by three parameters : the dynamic viscosity  $\mu$ , the relaxation  $\lambda_1^*$  and the retardation  $\lambda_2^*$  times. The relation  $Rv = \lambda_2^*/\lambda_1^*$  may also be used instead of  $\lambda_2^*$ .

In order to derive a macroscopic filtration law based on the Oldroyd constitutive equation, we have to introduce the filtration velocity  $\mathbf{V}^*$  defined by the Dupuit's equation :

$$\mathbf{V}^* = \phi \mathbf{U}^* \quad (6)$$

where  $\phi$  is the porosity. Substituting Equation 5 into 1 and using the REV method by averaging the resulting equation and taking into account Equation 6 defined by the Dupuit's equation :

$$\frac{\rho}{\phi} (1 + \lambda_1^* \frac{\partial}{\partial t^*}) \frac{\partial \mathbf{V}^*}{\partial t^*} + \frac{\mu}{K} (1 + \lambda_2^* \frac{\partial}{\partial t^*}) \mathbf{V}^* + (1 + \lambda_1^* \frac{\partial}{\partial t^*}) (\nabla P^* - \rho \mathbf{g}) = 0, \quad (7)$$

where  $K$  is the permeability.

Under the assumption of low Reynolds number based on the pore dimension, the generalized Darcy's law 7 is also derived by [12] using a homogenization theory.

The fluid density  $\rho$  obeys the state law :

$$\rho = \rho_0(1 - \beta_T(T^* - T_0^*)) \quad (8)$$

where  $\rho_0$  is the fluid density at temperature  $T_0^*$  and  $\beta_T$  is the thermal expansion coefficient. Energy and continuity equations can then be written as :

$$\frac{(\rho c)_{sf}}{(\rho c)_f} \frac{\partial T^*}{\partial t^*} + \mathbf{V}^* \cdot \nabla T^* = \nabla \cdot (\alpha \nabla T^*) \quad (9)$$

$$\nabla \cdot \mathbf{V}^* = 0 \quad (10)$$

The boundary conditions at the impermeable, perfectly conducting horizontal walls and the impermeable insulated walls are :

$$\begin{aligned} -k_T \frac{\partial T^*}{\partial z} &= q \quad \text{at} \quad z = 0, H, \\ \partial T^* / \partial x &= 0 \quad \text{at} \quad x = 0, W, \\ \partial T^* / \partial y &= 0 \quad \text{at} \quad y = 0, e, \\ \mathbf{V} \cdot \mathbf{n} &= 0 \quad \text{at} \quad \partial\Omega. \end{aligned} \quad (11)$$

here,  $k_T$ ,  $(\rho c)$ ,  $\alpha = k_T / (\rho c)_f$ ,  $\mu$ ,  $\nu$ , are respectively the effective thermal conductivity, the heat capacity per unit volume, the effective thermal diffusivity and the dynamic and kinematic viscosity of the fluid. Subscript (sf) refers to an effective quantity, while (f) refers to the fluid alone.

We choose  $H$ ,  $k_T / (H(\rho c)_f)$ ,  $H^2(\rho c)_{sf} / k_T$ ,  $k_T \mu / (K(\rho c)_f)$  and  $qH / k_T$  as reference quantities for length, velocity, time, pressure and temperature. With this scaling, the following set of dimensionless equations is obtained :

$$\nabla \cdot \mathbf{V} = 0 \quad (12)$$

$$(1 + \lambda_1 \frac{\partial}{\partial t}) \frac{1}{Pr_D} \frac{\partial \mathbf{V}}{\partial t} + (1 + Rv\lambda_1 \frac{\partial}{\partial t}) \mathbf{V} + (1 + \lambda_1 \frac{\partial}{\partial t})(\nabla P - RaT\mathbf{e}_z) = 0, \quad (13)$$

$$\frac{\partial T}{\partial t} + \mathbf{V} \cdot \nabla T = \nabla^2 T \quad (14)$$

The dimensionless boundary conditions are :

$$\begin{aligned} \frac{\partial T}{\partial z} &= -1 \quad \text{at} \quad z = 0, 1, \\ \partial T / \partial x &= 0 \quad \text{at} \quad x = \pm \frac{A}{2}, \\ \partial T / \partial y &= 0 \quad \text{at} \quad y = 0, a, \\ \mathbf{V} \cdot \mathbf{n} &= 0 \quad \text{at} \quad \partial\Omega. \end{aligned} \quad (15)$$

The Darcy-Prandtl number  $Pr_D$  is defined as  $Pr_D = (\phi Pr) / Da$ , with  $Da = K / H^2$  and  $Pr = \nu / k_T$ .

Since in the common porous media the Darcy number is very small, the Darcy-Prandtl number  $Pr_D$  takes quite large values. Therefore, the first term in Equation 13 is omitted in what follows. The remaining dimensionless parameters are : the filtration Rayleigh number

$$Ra = \frac{\beta_T g K H^2 q}{\alpha \nu k_T} \quad (16)$$

the horizontal and lateral aspect ratios

$$A = W/H, \quad a = e/H \quad (17)$$

the relaxation time

$$\lambda_1 = \lambda_1^* k_T / (H^2 (\rho c)_{sf}) \quad (18)$$

and the ratio  $Rv$  that varies in the interval  $[0, 1]$

$$Rv = \lambda_2^* / \lambda_1^* \quad (19)$$

This model reduces to the Maxwell model in the limit  $Rv \rightarrow 0$  and to the Newtonian model in the limit  $Rv \rightarrow 1$ .

In the following we will examine the instability of the conductive state (the primary instability) as well as the instability of the monocellular flow (the secondary instability).

### 3 Primary stationary and oscillatory instabilities

In the conductive regime, the basic solution is a motionless state  $\mathbf{V} = \mathbf{0}$  with a vertical thermal stratification  $T_0 = -z + \frac{1}{2}$ .

The aim of this section is to perform a temporal stability analysis of the conductive state with respect to both stationary and oscillatory disturbances.

To investigate the stability of the basic solution, infinitesimal three-dimensional perturbations are superimposed onto the basic solution :

$$\begin{cases} \mathbf{V} = \mathbf{V}_0 + \mathbf{v}(x, y, z, t) \\ T = T_0 + \theta(x, y, z, t) \\ P = P_0 + p(x, y, z, t) \end{cases} \quad (20)$$

We assume very large aspect ratios  $A (A \rightarrow \infty)$  and  $a (a \rightarrow \infty)$ . The three-dimensional disturbance quantities are expressed as

$$(u, v, w, \theta, p) = [\tilde{u}(z), \tilde{v}(z), \tilde{w}(z), \tilde{\theta}(z), \tilde{p}(z)] \exp(ikx + ily - i\omega t) \quad (21)$$

where  $k$  and  $l$  are the wave numbers in the  $x$  and  $y$  directions respectively, and the temporal growth rate of unstable perturbations is given by the imaginary part of the complex frequency  $\omega = \omega_r + i\omega_i$ . Therefore, the neutral temporal stability curve is obtained for  $\omega_i = 0$  which selects dominant modes at the onset of convection.

Substituting Equations (20)-(21) into (12)-(15), linearizing the equations and applying the curl twice to the momentum balance equation, one can obtain

$$(1 - i\omega Rv\lambda_1)(D^2 - \tilde{k}^2)\tilde{w} + Ra(1 - i\omega\lambda_1)\tilde{k}^2\tilde{\theta} = 0 \quad (22)$$

$$-i\omega\tilde{\theta} - \tilde{w} - (D^2 - \tilde{k}^2)\tilde{\theta} = 0 \quad (23)$$

where  $D = \frac{d}{dz}$  and  $\tilde{k}^2 = k^2 + l^2$ . The corresponding boundary conditions take the form

$$\tilde{w} = 0, \quad \frac{d\tilde{\theta}}{dz} = 0 \quad \text{at} \quad z = 0, 1. \quad (24)$$

The system (31) - (32) is solved by means of the Galerkin method using the following expansions

$$\tilde{w}(z) = \sum_{n=1}^M w_n \sin(n\pi z) \quad (25)$$

$$\tilde{\theta}(z) = \sum_{n=1}^M \theta_n \cos[(n-1)\pi z] \quad (26)$$

The number  $M$  of modes is chosen so that the quantitative convergence is secured.

As the viscoelastic parameters appear only in front of a time derivative in the momentum equation (16), the elasticity of the fluid cannot influence the properties of a stationary instability. Consequently, the characteristics of the stationary instability are the same as for Newtonian fluids. For such fluids, linear instability analysis has been considered by Nield [9] and has provided quantitative information on the stability condition when the porous layer is supposed infinite in  $x$  and  $y$  directions.

We first consider perturbations in the form of stationary convection. Having used the Galerkin expansion (25) - (26) with  $M = 5$ , we obtain results with a very good agreement with those obtained in [9]. Fig 1(a) represents the marginal stability curve in the  $(\tilde{k}, Ra)$  plane and shows that a long wave instability (i.e. the critical wave number  $\tilde{k}_c = 0$ ) may develop if the Darcy-Rayleigh number exceeds the critical value  $Ra^s = 12,009$  in accordance with the critical value  $Ra^s = 12$  found in [9].

It is well established that for isothermal horizontal boundaries, competition between the processes of stress relaxation, strain retardation and thermal diffusion may also lead to an oscillatory convective instability as a first bifurcation ([3]-[8]). This feature is also found in the actual study when the viscoelastic fluid saturating the porous layer is heated by a constant flux.

In Figure 1(b) we plot the curve of neutral stability for oscillatory mode of convection in the  $(\tilde{k}, Ra)$  plane for  $Rv = 0.02$  and different values of the elasticity number  $\lambda_1 = 0.4; 0.5; 0.6$ . It can be seen from this figure that the minimum value of Rayleigh number is lower than the critical Rayleigh number  $Ra = 12$  needed to trigger steady long wave instability. Therefore oscillatory instability may set up as a first convective pattern instead of steady long wave instability. The dependence of the critical Rayleigh number and the critical frequency at the onset of oscillatory convection on the elasticity number  $\lambda_1$  for fixed values of  $Rv$  is numerically determined and the results are plotted in Fig. 2(a) and in Fig. 2(b) respectively.

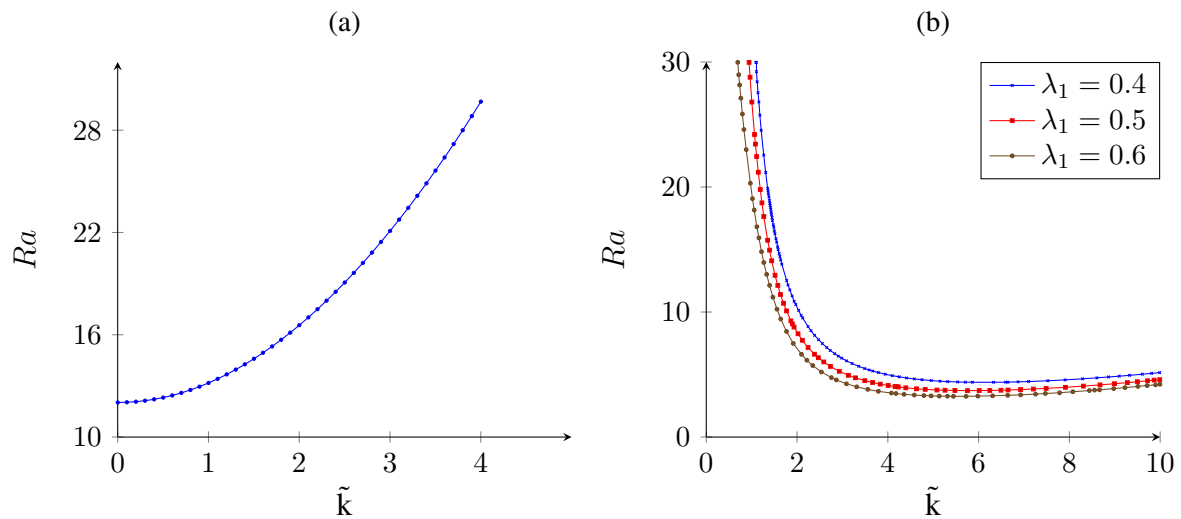


FIGURE 1 – Neutral stability curves : (a) stationary instability ; (b) oscillatory instability.

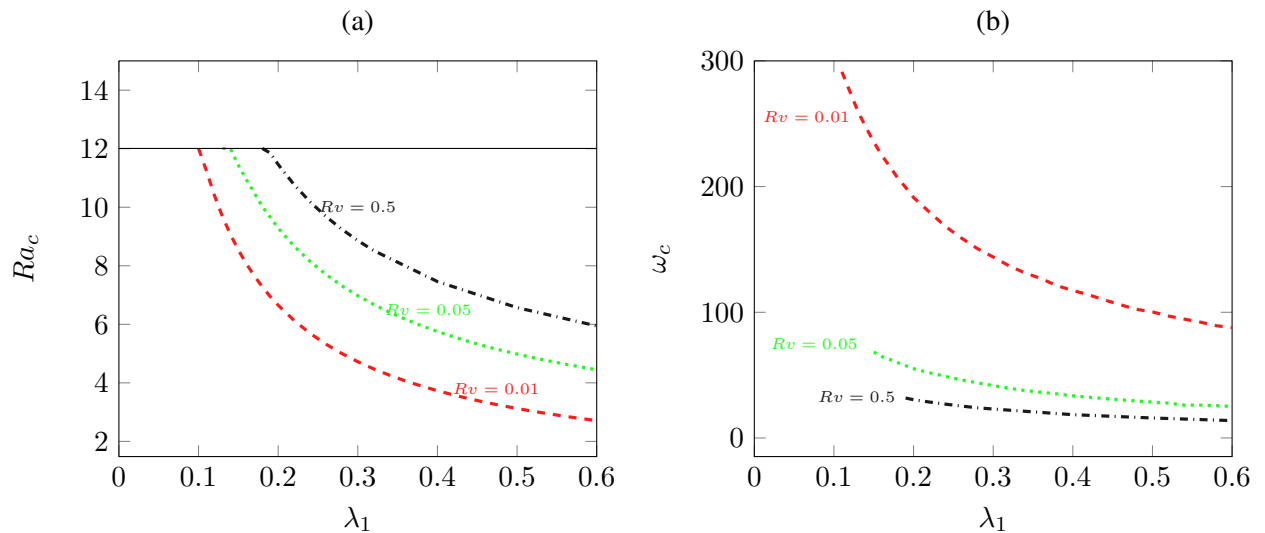


FIGURE 2 – (a) Critical Rayleigh number and (b) critical frequency at the onset of oscillatory convection as a function of  $\lambda_1$  for different values of  $Rv$ . The line  $Ra = 12$  in (a) corresponds to the critical Rayleigh number at the onset of stationary convection.

It is clear from 2(a) that an increase in  $\lambda_1$  leads to flow destabilization, i.e. to a reduction in the respective critical Rayleigh number. Fig. 2(a) also shows the stabilizing effect of the ratio  $Rv$ . Moreover, as it is seen in fig. 2(a), for a fixed value of  $Rv$ , there exists a particular value of  $\lambda_1 = \lambda_1^f$  where the critical Rayleigh numbers for the onsets of both oscillatory and stationary convection coincide and therefore a codimension two bifurcation occurs. For  $\lambda_1 > \lambda_1^f$ , Fig. 2(b) shows that the critical frequency decreases with the decrease of the fluid elasticity or the increase of the viscosity ratio.

## 4 Secondary instabilities

### 4.1 Nonlinear solution and formulation of its linear stability

According to above linear stability analysis, we found that a stationary bifurcation occurs giving rise to a convective pattern in the form of a long wave instability in the  $x$  direction provided that the elasticity number  $\lambda_1$  do not exceed a particular value  $\lambda_1^f$  which depends on the viscosity ratio  $Rv$ . In that case, the viscoelastic fluid behaves like a Newtonian fluid. Consequently, the nonlinear solution in the regime of steady long wave convection is the same regardless of whether or not the fluid is viscoelastic.

As shown by Bejan [13] for a vertical cavity, and later adopted by Vasseur et al. [14] and Sen et al. [15] for inclined cases, one may assume the existence of a two-dimensional and fully developed counterflow. This may be a good approximation for the mid-region of the horizontally extended space on condition that the unicellular convection is stable. By assuming a shallow cavity  $A \gg 1$  and by using the parallel flow approximation, Kimura et al. [2] found that the analytical solution for the monocellular flow consists of :

a horizontal asymmetric velocity with a zero mean along any vertical section,

$$U(z) = \frac{1}{2} Ra C (1 - 2z) \quad (27)$$

and a vertical as well as a horizontal stratification of the temperature,

$$T_0(x, y, z) = Cx + \Theta(z) \quad (28)$$

with

$$\Theta(z) = \frac{1}{2} Ra C^2 (z - z^2) - 1 \quad (29)$$

and

$$C = \pm \sqrt{\frac{10}{Ra} \left(1 - \frac{12}{Ra}\right)} \quad (30)$$

where  $C$  is negative or positive according to whether the flow is clockwise or counter-clockwise and both solutions are possible depending on the initial conditions.

From Equation (30) it is seen that no motion may be induced inside the cavity for  $Ra < 12$ . For the case of a porous medium heated from the bottom and cooled from the top by a constant heat flux, a critical Rayleigh number of  $Ra = 12$  for the onset of convection was predicted by Nield [9]. This result is in agreement with the prediction of Equation (30).

For finite aspect ratio, Kimura et al. [2] performed two dimensional numerical simulations of the full problem. Their numerical results show that the conductive state is stable when the Rayleigh number is smaller than 12. Computations carried out for  $Ra$  in excess of 12 were found to agree with analytical solutions (27 - 29).

The equations governing the linear stability of the monocellular flow are obtained by the same previous approach used for the stability of the conductive basic solution. By assuming very large aspect ratios



$A(A \rightarrow \infty)$  and  $a(a \rightarrow \infty)$  the following system is obtained

$$(1 - i\omega Rv\lambda_1)(D^2 - \tilde{k}^2)\tilde{w} + Ra(1 - i\omega\lambda_1)\tilde{k}^2\tilde{\theta} = 0 \quad (31)$$

$$-i\omega\tilde{\theta} + \tilde{w}DT_0 + ik\tilde{\theta}U_0 - (D^2 - \tilde{k}^2)\tilde{\theta} = 0 \quad (32)$$

where we substitute  $U_0$  and  $T_0$  by their explicit expressions (27) - (29).

The corresponding boundary conditions take the form

$$\tilde{w} = 0, \quad \frac{d\tilde{\theta}}{dz} = 0 \quad \text{at} \quad z = 0, 1. \quad (33)$$

On the other hand, if we assume a very large aspect ratio  $A$  and a finite value of the lateral aspect ratio  $a$  study by [16], the governing equations are still the system (31) - (32) where  $\tilde{k}^2$  is replaced by  $k^2 + L\pi/a^2$ .

The resulting linear stability problem is solved by means of the Galerkin method, using the expansion (25) - (26) at the order  $M = 30$ .

## 4.2 Results for Newtonian and viscoelastic fluids

To verify the accuracy of our numerical results based on the Galerkin expansion to the order  $M = 30$ , we perform a test for the limiting case of a Newtonian fluid and compare the results with those obtained by Kimura et al. [2]. In the first instance, two-dimensional disturbances, corresponding to  $l = 0$ , were considered. We found out that for the Newtonian fluid, the base velocity and temperature profiles (27) - (29) are stable for values of  $Ra$  less than  $Ra_{c2}^T = 506.27$  as shown by the neutral stability curve represented in Figure 3 (a). At this critical Rayleigh number occurs an instability via a Hopf bifurcation to oscillatory TRs with a critical frequency  $\omega_{c2}^T = 138.24$  and a critical wave number  $k_{c2}^T = 4.80$ . These results are in a good agreement with those obtained in [2] by using a shooting method, namely  $Ra_{c2}^T = 506.07$ ,  $\omega_{c2}^T = 138.92$  and  $k_{c2}^T = 4.82$ .

In order to study the influence of viscoelastic parameters on the secondary instability, we first computed the bifurcation line from a stationary monocellular convective pattern to oscillatory TRs ( $l = 0$ ) for either a fixed value of the elasticity number  $\lambda_1$  with varying values of the viscosity ratio  $Rv$  or a fixed value of  $Rv$  with varying values of  $\lambda_1$ . With regard to the question of the influence of the viscosity ratio  $Rv$  for a viscoelastic fluid with a relaxation time  $\lambda_1 = 0.1$  on the onset of a secondary instability in the form of oscillatory TRs, Figure 3 illustrates the behavior of neutral stability curves in the  $(k, Ra)$  plane for  $Rv = 0.75$ ,  $Rv = 0.5$  and  $Rv = 0.3$ . For a comparison, the Newtonian case ( $Rv = 1$ ) is also represented on figure 3.

We note in this figure that the minimum of neutral stability curves increases when  $Rv$  is augmented to reach the critical value for Newtonian fluids in the limit of  $Rv = 1$ . Physically, this result means that concentrated polymeric solutions with a small viscosity ratio  $Rv$  favor the appearance of oscillatory multicellular flow convection as a secondary instability. On the other hand, for diluted viscoelastic solutions, more heating is needed to trigger the secondary instability.

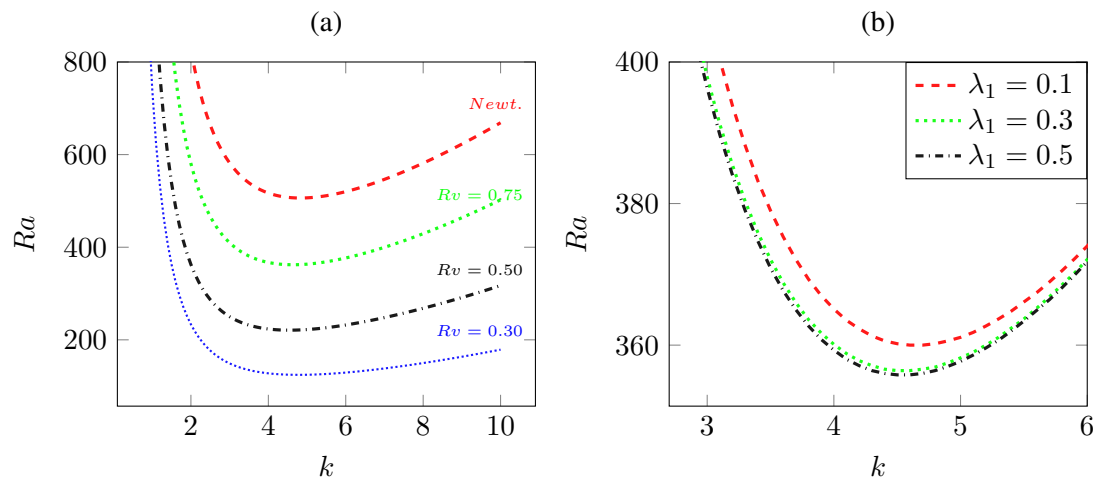


FIGURE 3 – Critical Rayleigh number for the destabilization of fully developed flow against the wave number  $k$  with  $l = 0$  for Newtonian fluids (Newt) and for viscoelastic solutions with  $\lambda_1 = 0.1$  and different values of the viscosity ratio  $Rv$ .

## 5 Conclusion

In the present paper, Galerkin method is used to investigate the primary and secondary instabilities of viscoelastic fluids saturating a porous layer heated from below by a constant flux. The modified Darcy's law based on the Oldroyd-B model was used for modeling the momentum equation. In addition to Darcy-Rayleigh number  $Ra$ , two viscoelastic parameters play a key role when characterizing the temporal behavior of the instability, namely, the relaxation time  $\lambda_1$  which measures the elasticity of the fluid and the ratio  $Rv$  between the viscosity of the solvent and the total viscosity of the fluid. In the first part of the paper, three-dimensional disturbances were considered in order to study the stability of the basic motionless solution. For sufficiently elastic fluids, we found that the primary instability is oscillatory. Otherwise, the primary bifurcation gives rise to stationary long wave instability. Based on a fully developed parallel flow assumption, a nonlinear analytical solution for the velocity and temperature fields was developed in the range of the rheological parameters where stationary long wave instability develops first. In the second part of the paper, we reported findings on the linear stability analysis of the monocellular flow which is performed with special attention given to the interplay between the viscoelastic parameters. For weakly elastic fluids we determined a second critical value of Rayleigh number above which the system exhibits a Hopf bifurcation from steady monocellular flow to oscillatory transverse rolls convection. The well known limit of  $Ra_{c2}^T \approx 506$  for Newtonian fluids is recovered and the fluid elasticity effect is found to delay the onset of the Hopf bifurcation.

## Références

- [1] Hirata, S. C. and Ella Eny, G and Ouarzazi, M. N. Nonlinear pattern selection and heat transfer in thermal convection of a viscoelastic fluid saturating a porous medium. *International Journal of Thermal Sciences* **2015**,95, 136–146.

- [2] Kimura, S. and Vynnycky, M. and Alavyoon, F. Unicellular natural circulation in a shallow horizontal porous layer heated from below by a constant flux. *Journal of Fluid Mechanics* **1995**, 294, 231–257.
- [3] Kim, M. C. and Lee, S. B. and Kim, S. and Chung, B. J. Thermal instability of viscoelastic fluids in porous media. *International journal of heat and mass transfer* **2003**, 46, 5065–5072.
- [4] Yoon, D. and Kim, M. C. and Choi, C. K. The onset of oscillatory convection in a horizontal porous layer saturated with viscoelastic liquid. *Transport in porous media* **2004**, 55, 275–284.
- [5] Hirata, S. C. and Ouarzazi, M. N. Three-dimensional absolute and convective instabilities in mixed convection of a viscoelastic fluid through a porous medium. *Physics Letters A* **2010**, 374, 2661–2666.
- [6] Alves, L.S. and Barletta, A. and Hirata, S. and Ouarzazi, M. N. Effects of viscous dissipation on the convective instability of viscoelastic mixed convection flows in porous media. *Int. J. Heat Mass Transfer* **2014**, 70, 586–598.
- [7] Delenda, N. and Hirata, S. C. and Ouarzazi, M. N. Primary and secondary instabilities of viscoelastic mixtures saturating a porous medium : Application to separation of species. *Journal of Non-Newtonian Fluid Mechanics* **2012**, 181, 11–21.
- [8] Taleb, A. and Ben Hamed, H. and Ouarzazi, M. N. and Beji, H. Analytical and numerical analysis of bifurcations in thermal convection of viscoelastic fluids saturating a porous square box. *Phys. Fluids* **2016**, 28, 053106.
- [9] Nield, D. A. Onset of thermohaline convection in a porous medium. *Water Resources Research* **1968**, 4, 553–560.
- [10] Skartsis, L. and Khomami, B. and Kardos, J. L. Polymeric flow through fibrous media. *Journal of Rheology* **1992**, 36, 589–620.
- [11] Joseph, Daniel D. Fluid dynamics of viscoelastic liquids. *Springer-Verlag New York* **1990**.
- [12] Khuzhayorov, B. and Auriault, J. L. and Royer, P. Derivation of macroscopic filtration law for transient linear viscoelastic fluid flow in porous media. *International Journal of Engineering Science* **2000**, 38, 487–504.
- [13] Bejan, A.. The boundary layer regime in a porous layer with uniform heat flux from the side. *International Journal of Heat and Mass Transfer* **1983**, 26, 1339–1346.
- [14] Vasseur, P. and Satish, M. G. and Robillard, L. Natural convection in a thin, inclined, porous layer exposed to a constant heat flux. *International Journal of Heat and Mass Transfer* **1987**, 30, 537–549.
- [15] Sen, M. and Vasseur, P. and Robillard, L. Multiple steady states for unicellular natural convection in an inclined porous layer *International journal of heat and mass transfer* **1987** 30 2097–2113.
- [16] Gueye, A. and Ouarzazi, M. and Hirata, S. and Ben Hamed, H., Onset of Primary and Secondary Instabilities of Viscoelastic Fluids Saturating a Porous Layer Heated from below by a Constant Flux, Preprints 2017 2017040013 (doi : 10.20944/preprints201704.0013.v1).